

Supplemental Information

1. Experimental setup

The experiments were performed with an ultrahigh-vacuum and low-temperature STM (type Unisoku USM-1300). All measurements were carried out at 0.5 K and with the external magnetic field aligned to the easy magnetic axis of the Fe atoms using a three-dimensional vector magnet. The PtIr-tip was prepared by sputtering with Argon and thermal flashing using electron-beam bombardment for several seconds. Lock-In detection was used to record the differential conductance, dI/dV , by adding an AC modulation voltage of $72 \mu\text{V}_{\text{RMS}}$ at 730.5 Hz to the bias voltage.

The Cu_2N substrate was prepared similarly to previous publications [2, 3]. The monoatomic Cu_2N layer was grown on a clean Cu(100) crystal. To clean the Cu crystal several cycles of Ar-sputtering and annealing at 850 K were performed. The monoatomic Cu_2N layer was prepared by sputtering with N_2 at 1 kV and annealing to 600 K. The Fe atoms were deposited on the precooled sample with a low flux of Fe vapor from a Knudsen cell. We confirmed that the sample temperature did not exceed 100 K during Fe dosing by replacing the sample with a temperature sensor.

2. Rates in the Pauli Master equation and spin Hamiltonian

The rates $r_{ij}^{k \leftarrow a \leftarrow m}$ are given by the product of the scattering Hamiltonian's transition matrix elements and the integral over all electron and hole states available for scattering in the electron baths of the two electrodes k and m .

$$r_{ij}^{k \leftarrow a \leftarrow m} = \frac{G^{k \leftarrow m}}{e} \sum_{\{\sigma, \sigma'\}=\{+, -\}} \iint d\epsilon d\epsilon' f(\epsilon) \left(1 - f(\epsilon' - eV^{k \leftarrow m})\right) \times \frac{(1 + \sigma\eta_k)(1 + \sigma'\eta_m)}{2} \times \left| \langle i, \sigma' | \hat{S}_a \hat{\sigma} + u \hat{I} | j, \sigma \rangle \right|^2 \delta(\epsilon - \epsilon' - \Delta\epsilon_{ij})$$

where $G^{k \leftarrow m}$ gives the conductance of the scattering channel. $V^{k \leftarrow m}$ is the voltage difference of the electrodes, η_k and η_m indicate their spin polarization. σ and σ' are $\pm \frac{1}{2}$ and represent the initial and final spin states of tunneling electrons, $f(\epsilon)$ is the Fermi distribution function and $\Delta\epsilon_{ij}$ is the energy difference between the two spin states $|i\rangle$ and $|j\rangle$. The spin state wave functions, $|j\rangle$, are extracted by exact diagonalization of an effective spin Hamiltonian with the form:

$$\hat{H}_{\text{trimer}} = \sum_{a=1}^3 \left[D_i \hat{S}_{z,a}^2 + E_i (\hat{S}_{x,a}^2 - \hat{S}_{y,i}^2) + g_a \mu_B \vec{B} \hat{S}_a \right] + \sum_{i=1}^2 J_{i(i+1)} \hat{S}_i \hat{S}_{i+1} + \hat{H}_{\text{tip}}$$

$$\hat{H}_{\text{tip}} = J_t \frac{\langle \vec{M}_t \rangle}{|\langle \vec{M}_t \rangle|} \hat{S}_1$$

where each of the three Fe atoms is described by the spin operators $\hat{S}_{x,a}$, $\hat{S}_{y,a}$ and $\hat{S}_{z,a}$ with spin quantum number $S = 2$ [3, 1]. The first term accounts for magneto-crystalline anisotropy and Zeeman splitting with D_a , E_a being the anisotropy parameters and g_a as the g-factor of the Fe atoms in Fe trimer. The second term is nearest-neighbor Heisenberg exchange interaction between the Fe atoms with strength $J_{a(a+1)}$. The last term describes the magnetic interaction between the side atom of the Fe trimer and the spin polarized STM tip, which is non-negligible at the vacuum gap sizes used in this work (J_t is the interaction strength and $\frac{\langle \vec{M}_t \rangle}{|\langle \vec{M}_t \rangle|}$ is the magnetization direction of the spin-polarized tip).

3. Fit routine

The routine used to fit the model to the data is explained here in more detail. The core of the fitting routine, a least squares method, is minimizing an error between calculated and experimental data, $E(\mathbf{P})$, as function of a parameter set \mathbf{P} . The list of parameters included in the set \mathbf{P} and their optimized values are listed in table S1. For the simulation the temperature was fixed to 0.5 K. The magnetic fields were fixed to 1 T or 2 T in the direction of the easy magnetic axis of Fe atoms. For all three Fe atoms the same $g_i = 2.1$ value was chosen [2].

The error between data and simulation is defined as follows:

$$E(\mathbf{P}) = \sum_{\sigma_{\text{set}} - 15mV}^{+15mV} \int dV \frac{\left(\frac{dI}{dV}_{\text{exp}, \sigma_{\text{set}}} - \frac{dI}{dV}(\mathbf{P})_{\text{sim}, \sigma_{\text{set}}} \right)^2}{\sigma_{\text{set}}^2}$$

In this error function, for each measured setpoint σ_{set} the differences between the simulated (sim) and experimental (exp) dI/dV spectra are squared, integrated over the investigated voltage regime and finally summed. To take the error from each setpoint into account evenly each dI/dV spectrum was normalized to its setpoint. In the fitting routine the full data set with 24 dI/dV spectra was used.

For a given fit parameter set \mathbf{P} the simulated dI/dV spectra for each setpoint are calculated according to the equations (1-4) in the main text. Since the tip interaction J_t and the coupling strengths G_{ml} depend on the setpoint they have to be adjusted to each setpoint. To adjust the tip interaction a power-law dependency with the two parameters A and χ was assumed:

$$J_t = A \left(\frac{\sigma_{\text{set}}}{\sigma_0} \right)^x$$

With $\sigma_0 = 0.433 \mu\text{S}$, which corresponds approximately to the setpoint at which the tip interaction is as large as the applied magnetic field. G_{ss} was kept constant for each setpoint, while G_{tt} was given by the coupling strength between tip and Cu substrate G_{st} and set to $G_{tt} = 0.5 G_{st}$. Finally G_{st} was adjusted in a way that the simulated current at 15 mV $I(15 \text{ mV})_{\text{sim}, \sigma_{\text{set}}}$ matches to the given setpoint σ_{set} :

$$\frac{I(15 \text{ mV}, G_{st})_{\text{sim}, \sigma_{\text{set}}}}{15 \text{ mV}} \stackrel{!}{=} \sigma_{\text{set}}$$

This approach assured that all fitting parameter effectively were independent of the setpoint σ_{set} .

Parameter	Best fit values
D_1, D_2, D_3 (meV)	-1.88(2), -2.42(1), -1.87(2)
E_1, E_2, E_3 (meV)	0.39(1), 0.20(5), 0.31(2)
J_{12}, J_{23} (meV)	0.71(2), 0.66(1)
η	0.58(6)
U	1.1(3)
G_{ss} (μS)	2.6(9)
A (T)	-0.95(5)
χ	1.1(1)

Table S1 The fit parameter set P used in the manuscript. The table also includes the optimized values of the fit parameters and their error.

4. Current-dependent $I(V)$ curves at 1T and 2T external magnetic field

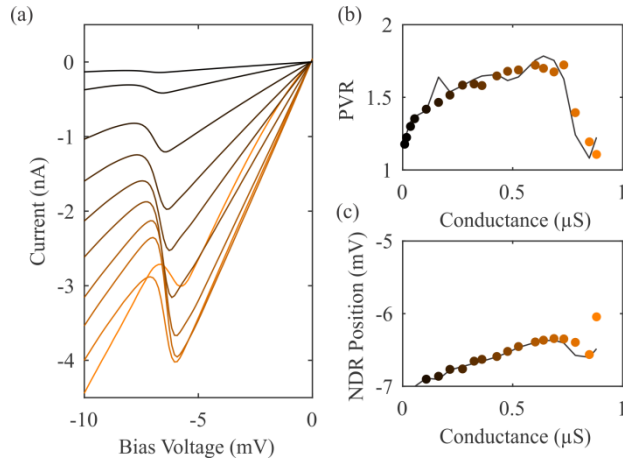


Figure S1 (a) Conductance-dependent $I(V)$ curves recorded with a spin-polarized tip on the side atom of the Fe trimer at 2 T external magnetic field. (b) Peak-to-valley ratio ($\text{PVR} = I_p/I_v$) as a function of setpoint conductance (colored points: experimental data, solid line: calculation). (c) Position of the NDR as a function of setpoint conductance (colored points: experimental data, solid line: calculation).

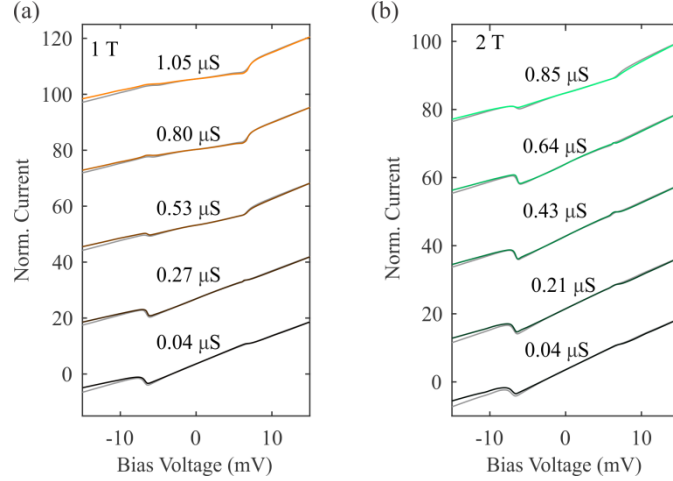


Figure S2 (a) Calculated (colored lines) and experimental (grey lines) conductance-dependent $I(V)$ curves for 1 T external magnetic field. (b) Conductance-dependent $I(V)$ curves for 2 T plotted analogous to (a)

5. Time evolution of the state occupation

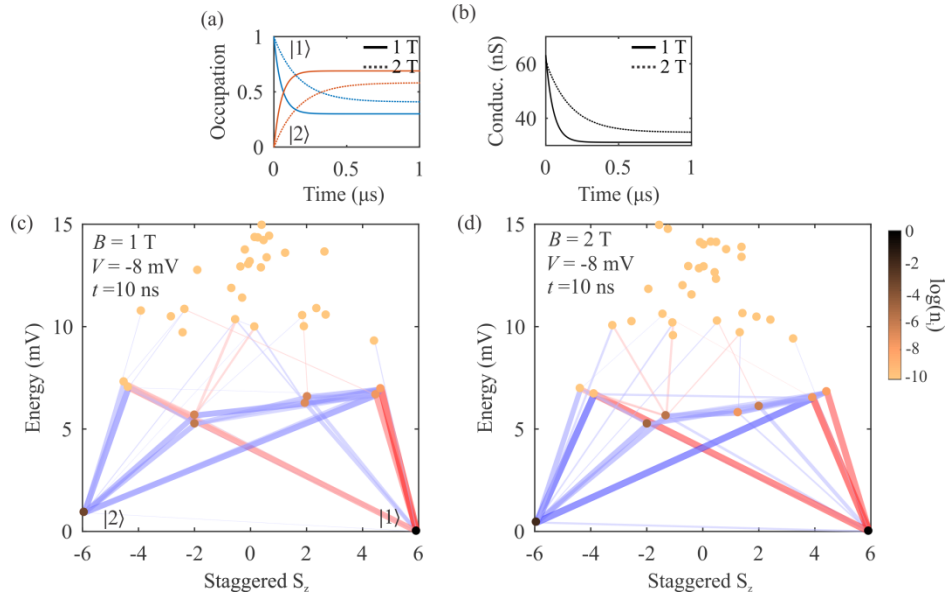


Figure S3 (a) Based on the rate equation model, the calculated temporal evolution of the two low-energy states ($|1\rangle$ and $|2\rangle$) of the Fe trimer by applying a voltage of -8 mV (starting from Boltzmann-distributed states occupation), with 1 T and 2 T applied external magnetic field. (b) After applying -8 mV bias voltage the total conductance decreases, since the high conductance state becomes less populated and the low conductance state more populated. ((c), (d)) The redistribution process at a time delay of 10 ns is shown in more detail, for 1 T (c) and 2 T (d) external magnetic field. The spin states are plotted as function of their eigenenergy and their staggered magnetization. The color of the dots indicates the occupation of the states. The red and blue lines show the most dominant excitation and de-excitation transitions between the spin states.

6. Resistance as function of voltage

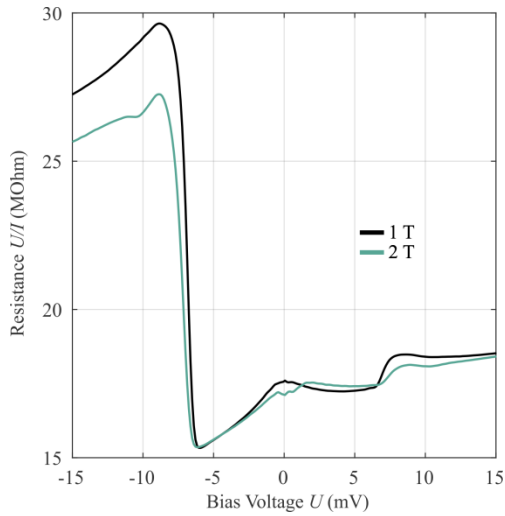


Figure S4 Resistance as function of voltage obtained from the $I(V)$ in Figure 3 (in the main text) for 1 T and 2 T magnetic field.

7. Spin polarized $I(V)$ curve and dI/dV spectrum recorded on the center atom of the Fe trimer

Figs. S5(a) and S5(b) show the measured and calculated $I(V)$ curves (Fig. S5(a)) and dI/dV spectra (Fig. S5(b)) on the center atom of Fe trimer. Fig. S5(c) shows the voltage-dependent occupation of the two low-energy states (state $|1\rangle$ and $|2\rangle$) of the Fe trimer when tunneling through the center atom. In the ground state (state $|1\rangle$), the magnetizations of the spin-polarized tip and the center atom of Fe trimer are antiparallel with each other. The efficient two-step excitation process described in the main text strongly populates state $|2\rangle$ starting at -7 mV. When tunneling through the center atom, state $|1\rangle$ is a low-conductance state and state $|2\rangle$ is a high-conductance state, hence increasing the occupation of state $|2\rangle$ does not cause NDR. And indeed, no NDR feature is observed at -7 mV on the center atom.

Surprisingly, an NDR feature appears at more negative bias of -10 mV (**Fig. S5a,b**). This behavior can be understood by inspecting the voltage-dependent occupation of the two low-energy spin states $|1\rangle$ and $|2\rangle$, Fig. S5c. At around -10 mV an excitation process through other excited spin states becomes possible and quickly depopulates state $|2\rangle$. This rapidly increases the occupation of state $|1\rangle$ which is a low-conductance state on the center atom, and an NDR feature appears.

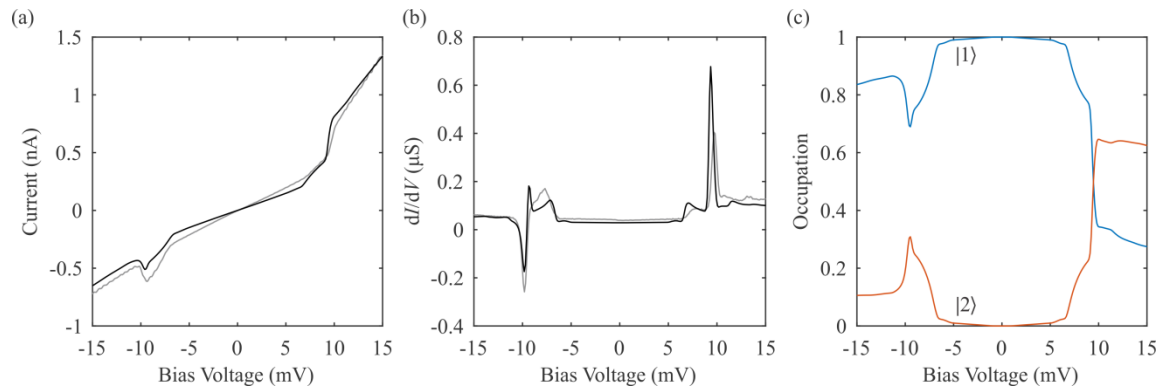


Figure S5 (a) Calculated (black) and measured (grey) spin polarized $I(V)$ curves on the center atom of the Fe trimer (setpoint of $0.089 \mu\text{S}$ at 2 T). (b) The corresponding dI/dV spectrum (black: calculated, grey: measured). (c) Calculated voltage-dependent occupation of the two low-energy states $|1\rangle$ and $|2\rangle$ when tunneling through the center atom of the Fe trimer.

References

- [1] Wolfgang Nolting and Anupuru Ramakanth. *Quantum theory of magnetism*. Springer Science & Business Media, 2009.
- [2] Shichao Yan, Deung-Jang Choi, Jacob A. J. Burgess, Steffen Rolf-Pissarczyk, and Sebastian Loth. Three-dimensional mapping of single-atom magnetic anisotropy. *Nano Letters*, 15(3):1938–1942, March 2015.
- [3] Shichao Yan, Deung-Jang Choi, Jacob A.J. Burgess, Steffen Rolf-Pissarczyk, and Sebastian Loth. Control of quantum magnets by atomic exchange bias. *Nature Nanotechnology*, 10(1):40–45, January 2015.